Available online at www.sciencedirect.com
SCIENCE DIRECT®
PERGAMON
International Journal of Heat and Mass Transfer 46 (2003) 4303–4317
International Journal of HEAT and MASS TRANSFER
www.elsevier.com/locate/ijhmt

Analytical characterisation of amplitude-dampening and phase-shifting in air/soil heat-exchangers

Pierre Hollmuller *

Centre universitaire d'étude des problèmes de l'énergie (CUEPE), Université de Genève, Battelle—bâtiment A, 7 route de Drize, CH-1227 Carouge, Genève, Switzerland

Received 20 September 2002; received in revised form 24 February 2003

Abstract

This article presents the complete analytical solution for the heat diffusion of a cylindrical air/soil heat-exchanger with adiabatic or isothermal boundary condition, submitted to constant airflow with harmonic temperature signal at input. It will be shown that, depending on its thickness, the soil layer will induce either one of two kinds of amplitude-dampening and phase-shifting regimes of the periodic input signal. In particular, for a thin layer submitted to adiabatic boundary condition, it is possible to completely phase-shift the periodic input while barely dampening its amplitude, a phenomenon apparently unexploited up to now, which might give rise to interesting energy handling techniques. Analytical results are validated against a finite-difference numerical simulation model as well as against an experimental setup.

Keywords: Modeling; Tubes; Ventilation

1. Introduction

1.1. State of the art

To the contrary of a liquid heat storage medium, which can generally be fairly well described by means of two separate conductivity and capacity parameters (one-node model), thermal exchange with a solid medium is of diffusive nature (conduction/capacitance continuum), inducing amplitude-dampening and phase-shifting of transient temperature input which are often difficult to predict intuitively. Lacking better tools, most authors [2,3,6,10,20,25,26,28–32] are dimensioning air/soil heat exchangers by way of simple static exchange models, simple to handle but for which estimation of the fundamental parameters (air/soil heat exchange coefficient and effective soil temperature) does not turn out evident, especially in transient regime.

Some analytical and semi-analytical approaches which explicitly treat heat diffusion in the soil actually concern steady-state problems. An elegant, approximate solution for water driven systems by Koschenz and Lehmann [18] in fact concerns the restraint geometry of pipe networks used within thin slabs (large inter-axial pipe distance, small distance to upper and lower free surfaces) and rather pursues to compute total heat flow and mean fluid temperature than temperature at pipe exit. Using conformal mapping, another approach by Chung et al. [7] explicitly treats air driven buried pipes in a semi-infinite medium (i.e. submitted to steady thermal linking with a free upper surface, without any other geometric restriction on heat diffusion). However, apart from treating geometric configurations different from those studied in this article, such steady-state approaches unfortunately do not account for phase-shifting effects.

One of the first analytical approaches concerning periodic heat diffusion from a cylindrical in semi-infinite medium embedded pipe is proposed by Claesson and Dunand [8]. It bases on the solution for an infinite medium, corrected by addition of a mirror sink above the

* Tel.: +41-22-705-9649; fax: +41-22-705-9639.
E-mail address: pierre.hollmuller@cuepe.unige.ch (P. Hollmuller).

0017-9310/$ - see front matter
doi:10.1016/S0017-9310(03)00199-6

Nomenclature

a_s	thermal diffusivity of soil (m^2/s)
c_a	thermal capacity of air (isobaric) (J/K kg)
c_s	thermal capacity of soil (J/K kg)
h	amplitude-dampening exchange coefficient of air/pipe + soil (W/K m^2)
h_a	convective exchange coefficient of air/pipe (W/K m^2)
h_s	amplitude-dampening exchange coefficient of soil (W/K m^2)
h_δ	amplitude-dampening exchange coefficient of soil, thickness δ, steady-state (W/K m^2)
h_Γ	combined amplitude-dampening and phase-shifting exchange coefficient ($h^*_\Gamma = h_s + ik_s$) (W/K m^2)
k	phase-shifting exchange coefficient of air/pipe + soil (W/K m^2)
k_s	phase-shifting exchange coefficient of soil (W/K m^2)
$\dot{m}_a$	airflow (kg/s)
Nu	Nusselt number (–)
Pr	Prandtl number
r	radial distance (m)
r_0	radius of pipe (m)
R_0	radius of pipe + soil (m)
Re	Reynolds number (–)
t	time (s)
S	exchange surface (m^2)
S_δ	characteristic exchange surface for soil of thickness δ, steady-state signal (m^2)
T_a	temperature of air (°C)
T_{a0}	temperature of air at input, steady state (°C)
T_s	temperature of soil (°C)
T_{s0}	temperature of soil at isothermal boundary, steady state (°C)
v_a	velocity of air (m/s)
x	length (m)
y	width (flat heat-exchanger) (m)

Greek symbols

δ	depth of heat penetration (m)
Δh	correction on amplitude-dampening exchange coefficient of air/pipe + soil (W/K m^2)
Δk	correction on phase-shifting exchange coefficient of air/pipe + soil (W/K m^2)
ΔR_0	thickness of soil ($\Delta R_0 = R_0 - r_0$) (m)
Δt	transit time within pipe (s)
θ_a	temperature amplitude of air (K)
θ_{a0}	temperature amplitude of air at input, harmonic state (K)
θ_s	temperature amplitude of soil, at pipe level (K)
Γ_s	temperature amplitude in soil, radial modulation (–)
λ_a	thermal conductivity of air (W/K m)
λ_s	thermal conductivity of soil (W/K m)
μ_a	viscosity of air (kg/m s)
ρ_a	density of air (kg/m^3)
ρ_s	density of soil (kg/m^3)
τ	period of temperature oscillation (s)
ω	Frequency of temperature oscillation (rad/s)

Others

–	an asterix signifies a complex value
–	a tilda signifies a dimensionless value, as defined in a specific section of the text

free surface and yields the solution for the temperature field in the soil. The induced effect on the longitudinal temperature variation of the airflow has been completed by Sawhney and Mahajan [27], appropriate physical interpretation and operational presentation of the results unfortunately not having been carried out. Apart from the thermal link with the upper plane surface (considered way above the penetration depth and submitted to phase-shifted periodic excitation), within latter studies heat diffusion however virtually extends over an infinite region, i.e. without restriction on available soil, and does hence not allow to detect the potential of complete phase-shifting that will be put forward within this work. A similar but somehow more complex problem including the interference of neighbouring pipes is proposed by Kabashnikov et al. [17], but also concerns deeply buried pipes and does not either discuss the effect of phase-shifting.

All preceding analytical approaches use simplifications which will also be assumed within this work. In particular, they do not account for axial conduction within soil or for axial dispersion of fluid, as do some similar studies on single-blow techniques [21,22], nor do they account for inhomogenous flow characteristics perpendicularly to axis.

As an alternative to the analytical approach, several numerical simulation models based on finite differences have also contributed to characterize diffusive heat exchangers. Some of them are limited to description of one only "typical" pipe [4,16,24]. Other ones allow for the description of several parallel running pipes, with or without possibility to treat more complicated cases than steady flow rate, homogenous and laterally adiabatic soils, or sole sensible heat exchange [5,9,11,13]. However, when validation against monitoring is ever carried out, latter in all cases remains limited to a few hours or

days and does generally not concern real scale installations, thereby not providing necessary proof of robustness one would expect. Corroboration against an analytical solution is furthermore never given, except for the last one of these models and for the trivial case of one-dimensional heat diffusion without airflow.

Probably the most worked out finite differences numerical model is that of Hollmuller and Lachal [14], allowing for variation in airflow rate and direction, inhomogeneous soils, non-adiabatic lateral boundary conditions, as well as description of latent heat exchanges and thermal effect of charge losses. Coherent with analytical approach to be developed hereafter, lateral heat convection within a pipe section is treated by means of an overall coefficient and velocity profile is considered to be uniform, while heat diffusion in soil is treated three-dimensionally. Extensive validation against several long-term monitored real scale installations already proved good robustness [15], but as for all other models, corroboration with an analytical solution was still missing up to now.

1.2. Objectives

As a response to the preceding state of the art and as part of a wider work on air/soil heat exchangers [15], this article will treat a problem similar to that attended by Sawhney and Mahajan [27], dropping the constraint of a free upper surface, but adding an isothermal or adiabatic boundary condition at finite radial distance (limitation of available soil layer). In a first step it will be shown that, depending on its thickness, the soil layer will induce either one of two kinds of amplitude-dampening and phase-shifting regimes. In particular, for a thin layer submitted to adiabatic boundary condition, it is possible to completely phase-shift the periodic input while barely dampening its amplitude, a phenomenon apparently unexploited up to now. Latter surprising result will finally be validated against numerical simulation with the model previously developed by the author, as well as against an experimental setup.

2. Cylindrical air/soil heat-exchanger

2.1. Problem definition

We consider a constant mass flow of air (or by extension any other fluid) submitted to sinusoidal temperature oscillation at entrance of a cylindrical pipe, itself embedded in a finite cylindrical soil layer with adiabatic or isothermal boundary condition (Fig. 1). Following hypothesis will further be made:

- In relation to perpendicular heat diffusion, longitudinal one is considered to be secondary and will hence not be accounted for. As will be seen by comparison with numerical simulation, this hypothesis will be more than good enough, at least as long as the characteristic length of amplitude-dampening or phase-shifting remains larger than the natural penetration depth.
- Within a given section air is considered to be homogenous, so that the dynamic of convective air/soil heat exchange will not be described in detail but by means of a unique convective heat exchange coefficient between airflow and pipe, supposed to be constant over the whole pipe length. Velocity profile is furthermore supposed to be uniform, so that bulk and average temperatures in a pipe section can be said to coincide. Comparison with experimental data as well as with a numerical model (itself validated against several

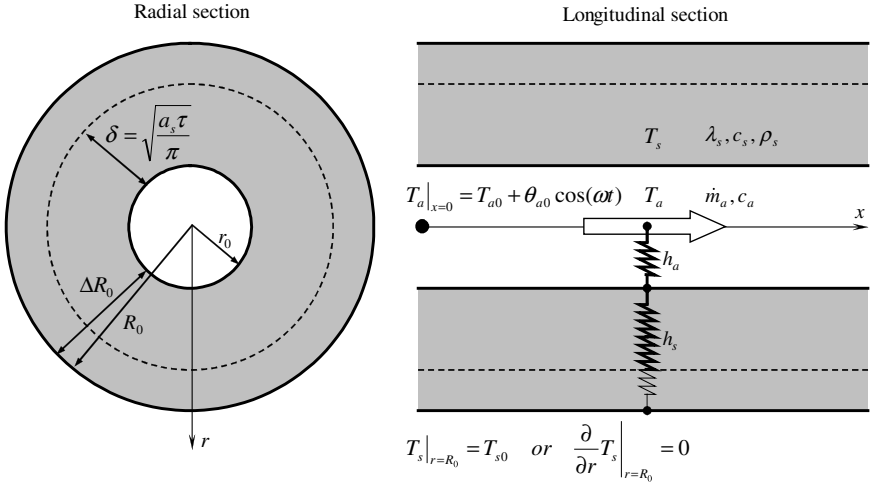

Fig. 1. Schematic of cylindrical air/soil diffusive heat exchanger.

in situ monitored real scale systems) should support for these assumptions to cause negligible errors in practical applications.

- Soil thermal conductivity and capacity are considered to be homogenous and constant, variation of soil type and water content not being accounted for. Nor is being considered any water movement inducing convective heat exchange within the soil.
- The pipe itself is not taken into account. In first approximation this hypothesis could if necessary be corrected by: (1) including the conductivity of the pipe into the convective heat exchange coefficient between airflow and pipe; (2) considering an effective soil radius which takes into account the pipe's thermal capacity.
- Possible latent heat exchanges are not accounted for, which means that no water infiltration is at work and that the air temperature is supposed to remain above its dew point.
- Thermal effect of charge losses are not taken into account.

This being, perfect radial conditions as considered here do usually not arise in practical situation, so that the radial limitation should be seen as an effective radius, bearing such limitative factors as the distance between parallel running pipes (adiabatic condition) or the presence of upper/lower building/ground water (isothermal condition). We will here not seek to give general means of adequately represent a real geometry in such a simplified form, but rather to use this simplified form to derive general insight on the behaviour of air/soil heat exchangers.

2.2. Mathematical formulation

The thermal exchanges of the system are governed by the following three differential equations, which respectively describe diffusion in the soil, convective air/soil exchange and the link between both at the pipe's level:

$$a_s\left(\frac{\partial^2 T_s}{\partial r^2}+\frac{1}{r}\frac{\partial T_s}{\partial r}\right)=\frac{\partial T_s}{\partial t} \tag{1}$$

$$c_a\dot{m}_a\left(\frac{\partial T_a}{\partial x}+\frac{1}{v_a}\frac{\partial T_a}{\partial t}\right)=2\pi r_0 h_a(T_s|_{r=r_0}-T_a) \tag{2}$$

$$\lambda_s\left.\frac{\partial T_s}{\partial r}\right|_{r=r_0}=h_a(T_s|_{r=r_0}-T_a) \tag{3}$$

Note that by appropriate rearrangement of (3), both the first equations can be written in function of T_s only, the third one yielding simple link to T_a:

$$a_s\left(\frac{\partial^2 T_s}{\partial r^2}+\frac{1}{r}\frac{\partial T_s}{\partial r}\right)=\frac{\partial T_s}{\partial t} \tag{4}$$

$$\left(\frac{\partial}{\partial x}+\frac{1}{v_a}\frac{\partial}{\partial t}\right)\left(T_s-\frac{\lambda_s}{h_a}\frac{\partial T_s}{\partial r}\right)\Bigg|_{r=r_0}-\frac{2\pi r_0}{c_a\dot{m}_a}\lambda_s\left.\frac{\partial T_s}{\partial r}\right|_{r=r_0}=0 \tag{5}$$

$$T_a=\left(T_s-\frac{\lambda_s}{h_a}\frac{\partial T_s}{\partial r}\right)\Bigg|_{r=r_0} \tag{6}$$

Dependence of a_s and v_a on other parameters is given by:

$$a_s=\frac{\lambda_s}{c_s\rho_s} \tag{7}$$

$$v_a=\frac{\dot{m}_a}{\rho_a\pi r_0^2} \tag{8}$$

while that of h_a will depend on the value of the Reynolds number:

$$Re=\frac{\rho_a v_a}{\mu_a}2r_0 \tag{9}$$

For laminar flow h_a may be considered to be independent of Re and thus of air velocity, which is not the case for turbulent flow anymore [19]:

$$h_a=\frac{\lambda_a}{2r_0}Nu \quad \text{with } Nu=\begin{cases}4.36 & (Re<2300)\\ 0.023Re^{0.8}Pr^{0.33} & (Re>10,000)\end{cases} \tag{10}$$

A refined formulation of latter form is also developed by Gnielinski [12], taking into account length to diameter as well as air to pipe temperature ratios, whereas for engineering purposes a roughly accurate linear form in function of v_a may also be used [15].

Finally, soil boundary condition will be either isothermal or adiabatic:

$$T_s|_{r=R_0}=T_{s0} \quad \text{or} \quad \left.\frac{\partial T_s}{\partial r}\right|_{r=R_0}=0 \tag{11}$$

and input air temperature is considered to be of a steady harmonic form:

$$T_a|_{x=0}=T_{a0}+\theta_{a0}\cos(\omega t) \tag{12}$$

Keeping in mind the linearity of (4)–(6), which allows for addition of distinct conditions/solutions, we will however seek separate solutions for the steady input (driven by T_{a0} and eventually T_{s0}) and for the harmonic component (driven by θ_{a0}).

2.3. Steady-state case

Before dealing with the periodic case we are most interested in, we will solve the steady-state, whose resolution as well as result will be used as a reference case. It is defined by following input and boundary conditions:

$$T_a|_{x=0} = T_{a0} \tag{13}$$

$$T_s|_{r=R_0} = T_{s0} \quad \text{or} \quad \left.\frac{\partial T_s}{\partial r}\right|_{r=R_0} = 0 \tag{14}$$

2.3.1. Uncoupling of geometric components

In steady-state regime T_s and T_a do not depend on t and we may proceed by separation of radial and longitudinal components, as follows:

$$T_s(x,r) = T_{s0} + \theta_s(x) \cdot \Gamma_s(r) \tag{15}$$

$$T_a(x) = T_{s0} + \theta_a(x) \tag{16}$$

Since θ_s and Γ_s are not defined in a unique way (multiplication by any constant and its inverse constituting another set of solution), we may arbitrarily impose following additional condition:

$$\Gamma_s|_{r=r_0} = 1 \tag{17}$$

which fixes θ_s as being the pipe temperature (temperature of the soil at $r = r_0$).

Using (15) and (16) and further defining:

$$h_\Gamma = \lambda\left(-\frac{1}{\Gamma_s}\frac{d\Gamma_s}{dr}\right)\bigg|_{r=r_0} \tag{18}$$

the original system (4)–(6) can then be written as:

$$\frac{\partial^2\Gamma_s}{\partial r^2} + \frac{1}{r}\frac{\partial\Gamma_s}{\partial r} = 0 \tag{19}$$

$$\frac{\partial\theta_s}{\partial x} + \frac{2\pi r_0}{c_a\dot{m}_a}\frac{h_a h_\Gamma}{h_a + h_\Gamma}\cdot\theta_s = 0 \tag{20}$$

$$\theta_a = \frac{h_a + h_\Gamma}{h_a}\cdot\theta_s \tag{21}$$

boundary conditions (13) and (14) becoming:

$$\theta_a|_{x=0} = T_{a0} - T_{s0} \tag{22}$$

$$\Gamma_s|_{r=R_0} = 0 \quad \text{or} \quad \left.\frac{d\Gamma_s}{dr}\right|_{r=R_0} = 0 \tag{23a,b}$$

2.3.2. Longitudinal solution

Trivial solution of (20), its link to (21) and boundary condition (22) allow to determine following longitudinal solutions:

$$\theta_s(x) = \frac{h_a}{h_a + h_\Gamma}(T_{a0} - T_{s0})\exp\left(-\frac{2\pi r_0}{c_a\dot{m}_a}\frac{h_a h_\Gamma}{h_a + h_\Gamma}x\right) \tag{24}$$

$$\theta_a(x) = (T_{a0} - T_{s0})\exp\left(-\frac{2\pi r_0}{c_a\dot{m}_a}\frac{h_a h_\Gamma}{h_a + h_\Gamma}x\right) \tag{25}$$

2.3.3. Radial solution

Submitted to condition (17), the general solution of (19) can be written as:

$$\Gamma_s(r) = \frac{\ln(Ar)}{\ln(Ar_0)} \tag{26}$$

where A is to be determined by one of the radial boundary conditions (23a,b).

- With the isothermal condition (23a) $A = R_0^{-1}$, so that (26) and (18) become

$$\Gamma_s(r) = \frac{\ln\left(\frac{r}{R_0}\right)}{\ln\left(\frac{r_0}{R_0}\right)} \tag{27a}$$

$$h_\Gamma = \frac{\lambda_s}{r_0\ln\left(\frac{R_0}{r_0}\right)} \tag{28a}$$

- With the adiabatic condition (19b) A tends to infinity, so that (26) and (18) become

$$\Gamma_s(r) = 1 \tag{27b}$$

$$h_\Gamma = 0 \tag{28b}$$

2.3.4. Complete solution

Defined by (15) and (16), the complete solution finally written as the product of the partial solutions (24), (25) and (27):

- With an isothermal boundary condition, one gets an exponential dampening of the input signal:

$$T_a(x) = T_{s0} + (T_{a0} - T_{s0})\exp\left(-\frac{2\pi r_0}{c_a\dot{m}_a}hx\right) \tag{29}$$

where the effective exchange coefficient h is given by serial linking of the convective and diffusive resistances of air and soil:

$$h = \frac{h_a h_s}{h_a + h_s} \tag{30}$$

and where the diffusive soil coefficient h_s is given by identification with h_Γ (28a).

With its thermal tension divided by the presence of h_a, the same exponential dampening arises along the soil, linked to a radial dampening of logarithmic type:

$$T_s(x,r) = T_{s0} + \frac{h_a}{h_a + h_s}\frac{\ln\left(\frac{r}{R_0}\right)}{\ln\left(\frac{r_0}{R_0}\right)}\cdot(T_{a0} - T_{s0}) \times \exp\left(-\frac{2\pi r_0}{c_a\dot{m}_a}hx\right) \tag{31}$$

- With an adiabatic boundary condition, one gets the trivial solution:

$$T_a(x) = T_s(x,r) = T_{a0} \tag{32}$$

corresponding to thermal saturation of the soil, which does not exchange anything with the airflow anymore.

2.4. Harmonic case

The harmonic case is on its turn defined by following input and boundary conditions:

$$T_a|_{x=0} = \theta_{a0}\cos(\omega t) \tag{33}$$

$$T_s|_{r=R_0} = 0 \quad \text{or} \quad \left.\frac{\partial T_s}{\partial r}\right|_{r=R_0} = 0 \tag{34}$$

It can be solved much in the same manner as before.

2.4.1. Uncoupling of time and geometric components

In harmonic steady-state regime we will seek a solution by using a complex notation:

$$T_a = Re\left[\theta_a^*(x)\exp(i\omega t)\right] \tag{35}$$

$$T_s = Re\left[\theta_s^*(x)\Gamma_s^*(r)\exp(i\omega t)\right] \tag{36}$$

which enables formal uncoupling of space and time variables, phase-shifts being carried by the argument of complex amplitudes θ_a^*, θ_s^* and Γ_s^*. Again we will fix θ_s^* to be the pipe's temperature, by imposing following additional condition:

$$\Gamma_s^*|_{r=r_0} = 1 \tag{37}$$

and will define:

$$h_\Gamma^* = \lambda\left(-\frac{1}{\Gamma_s^*}\frac{d\Gamma_s^*}{dr}\right)\bigg|_{r=r_0} \tag{38}$$

The original system (4)–(6) can then be written as:

$$\frac{\partial^2\Gamma_s^*}{\partial r^2} + \frac{1}{r}\frac{\partial\Gamma_s^*}{\partial r} = i\frac{\omega}{a_s}\Gamma_s^* \tag{39}$$

$$\frac{\partial\theta_s^*}{\partial x} + \left(i\frac{\omega}{v_a} + \frac{2\pi r_0}{c_a\dot{m}_a}\frac{h_a h_\Gamma^*}{h_a + h_\Gamma^*}\right)\cdot\theta_s^* = 0 \tag{40}$$

$$\theta_a^* = \frac{h_a + h_\Gamma^*}{h_a}\cdot\theta_s^* \tag{41}$$

boundary conditions (33) and (34) becoming:

$$\theta_a^*|_{x=0} = \theta_{a0} \tag{42}$$

$$\Gamma_s^*|_{r=R_0} = 0 \quad \text{or} \quad \left.\frac{d\Gamma_s^*}{dr}\right|_{r=R_0} = 0 \tag{43a,b}$$

2.4.2. Longitudinal solution

Just as before, trivial solution of (40), its link to (41) and boundary condition (42) allow to determine following longitudinal solutions:

$$\theta_s^*(x) = \frac{h_a}{h_a + h_\Gamma^*}\theta_{a0}\exp\left(-i\omega\Delta t - \frac{2\pi r_0}{c_a\dot{m}_a}\frac{h_a h_\Gamma^*}{h_a + h_\Gamma^*}x\right) \tag{44}$$

$$\theta_a^*(x) = \theta_{a0}\exp\left(-i\omega\Delta t - \frac{2\pi r_0}{c_a\dot{m}_a}\frac{h_a h_\Gamma^*}{h_a + h_\Gamma^*}x\right) \tag{45}$$

where Δt represents the transit time of the airflow over distance x:

$$\Delta t = \frac{x}{v_a} \tag{46}$$

2.4.3. Radial solution

The general solution of (39) can be written as:

$$\Gamma_s^*(r) = A_I I_0\left((1+i)\frac{r}{\delta}\right) + A_K K_0\left((1+i)\frac{r}{\delta}\right) \tag{47}$$

where δ represents the penetration depth proper to the soil diffusivity and the signal frequency:

$$\delta = \sqrt{\frac{2a_s}{\omega}} = \sqrt{\frac{a_s\tau}{\pi}} \tag{48}$$

and where I_n and K_n are modified Bessel functions of order n [1]. Using the derivation rules for Bessel functions, coefficients A_I and A_K are determined by means of (37) and one of the boundary conditions (43a,b). By further use of (38) one finally gets:

- With the isothermal condition (43a):

$$\Gamma_s^*(r) = \frac{I_0\left((1+i)\frac{r}{\delta}\right)\cdot K_0\left((1+i)\frac{R_0}{\delta}\right) - K_0\left((1+i)\frac{r}{\delta}\right)\cdot I_0\left((1+i)\frac{R_0}{\delta}\right)}{I_0\left((1+i)\frac{r_0}{\delta}\right)\cdot K_0\left((1+i)\frac{R_0}{\delta}\right) - K_0\left((1+i)\frac{r_0}{\delta}\right)\cdot I_0\left((1+i)\frac{R_0}{\delta}\right)} \tag{49a}$$

$$h_\Gamma^* = \frac{\lambda}{\delta}\cdot(1+i)\cdot(-1)\cdot\frac{I_1\left((1+i)\frac{r_0}{\delta}\right)\cdot K_0\left((1+i)\frac{R_0}{\delta}\right) + K_1\left((1+i)\frac{r_0}{\delta}\right)\cdot I_0\left((1+i)\frac{R_0}{\delta}\right)}{I_0\left((1+i)\frac{r_0}{\delta}\right)\cdot K_0\left((1+i)\frac{R_0}{\delta}\right) - K_0\left((1+i)\frac{r_0}{\delta}\right)\cdot I_0\left((1+i)\frac{R_0}{\delta}\right)} \tag{50a}$$

- With the adiabatic condition (43b):

$$\Gamma_{\mathrm{s}}^{*}(r)=\frac{I_0\left((1+\mathrm{i})\frac{r}{\delta}\right)\cdot K_1\left((1+\mathrm{i})\frac{R_0}{\delta}\right)+K_0\left((1+\mathrm{i})\frac{r}{\delta}\right)\cdot I_1\left((1+\mathrm{i})\frac{R_0}{\delta}\right)}{I_0\left((1+\mathrm{i})\frac{r_0}{\delta}\right)\cdot K_1\left((1+\mathrm{i})\frac{R_0}{\delta}\right)+K_0\left((1+\mathrm{i})\frac{r_0}{\delta}\right)\cdot I_1\left((1+\mathrm{i})\frac{R_0}{\delta}\right)} \tag{49b}$$

$$h_{\Gamma}^{*}=\frac{\lambda}{\delta}\cdot(1+\mathrm{i})\cdot(-1)\cdot\frac{I_1\left((1+\mathrm{i})\frac{r_0}{\delta}\right)\cdot K_1\left((1+\mathrm{i})\frac{R_0}{\delta}\right)-K_1\left((1+\mathrm{i})\frac{r_0}{\delta}\right)\cdot I_1\left((1+\mathrm{i})\frac{R_0}{\delta}\right)}{I_0\left((1+\mathrm{i})\frac{r_0}{\delta}\right)\cdot K_1\left((1+\mathrm{i})\frac{R_0}{\delta}\right)+K_0\left((1+\mathrm{i})\frac{r_0}{\delta}\right)\cdot I_1\left((1+\mathrm{i})\frac{R_0}{\delta}\right)} \tag{50b}$$

2.4.4. Complete solution

Defined by (35) and (36), the complete solution finally writes as the product of the partial solutions (44), (45) and (49) which only the real part should be taken. Hence, after decomposition in real and imaginary parts of the link which occurs between h_{a} and h_{Γ}^{*}:

$$\frac{h_{\mathrm{a}}h_{\Gamma}^{*}}{h_{\mathrm{a}}+h_{\Gamma}^{*}}=h+\mathrm{i}k \tag{51}$$

the air output temperature in steady-state oscillation can explicitly be written in terms of amplitude-dampening and phase-shifting of the input signal:

$$T_{\mathrm{a}}(x,t)=\theta_{\mathrm{a}0}\cdot\exp\left(-\frac{2\pi r_0}{c_{\mathrm{a}}\dot{m}_{\mathrm{a}}}hx\right)\cdot\cos\left(\omega\left(t-\frac{x}{v_{\mathrm{a}}}\right)-\frac{2\pi r_0}{c_{\mathrm{a}}\dot{m}_{\mathrm{a}}}kx\right) \tag{52}$$

Explicit evaluation of the coefficients h and k in (46) occurs by decomposition of h_{Γ}^{*} in real and imaginary parts:

$$h_{\Gamma}^{*}=h_{\mathrm{s}}+\mathrm{i}k_{\mathrm{s}} \tag{53}$$

which can be done by substituting the Bessel functions occurring in (50) by their approximating series [1]. With this definition, (51) may explicitly be written as follows:

$$h=\frac{h_{\mathrm{a}}h_{\mathrm{s}}}{h_{\mathrm{a}}+h_{\mathrm{s}}}+\Delta h \tag{54}$$

$$k=\frac{h_{\mathrm{a}}k_{\mathrm{s}}}{h_{\mathrm{a}}+h_{\mathrm{s}}}+\Delta k \tag{55}$$

$$\Delta h=(+)\frac{h_{\mathrm{a}}^2k_{\mathrm{s}}^2}{(h_{\mathrm{a}}+h_{\mathrm{s}})(h_{\mathrm{a}}^2+2h_{\mathrm{a}}h_{\mathrm{s}}+h_{\mathrm{s}}^2+k_{\mathrm{s}}^2)}\quad\text{with }\lim_{h_{\mathrm{a}}\to\infty}\Delta h=0 \tag{56}$$

$$\Delta k=(-)\frac{h_{\mathrm{a}}k_{\mathrm{s}}(h_{\mathrm{a}}h_{\mathrm{s}}+h_{\mathrm{s}}^2+k_{\mathrm{s}}^2)}{(h_{\mathrm{a}}+h_{\mathrm{s}})(h_{\mathrm{a}}^2+2h_{\mathrm{a}}h_{\mathrm{s}}+h_{\mathrm{s}}^2+k_{\mathrm{s}}^2)}\quad\text{with }\lim_{h_{\mathrm{a}}\to\infty}\Delta k=0 \tag{57}$$

At least in case of good convective heat exchange (large values of h_{a}), the amplitude-dampening coefficient h hence essentially turns out to be determined by serial linking of the convective coefficient h_{a} with the diffusive coefficients h_{s}, while a very similar relation between h_{a}, h_{s} and k_{s} determines the phase-shifting coefficient k.

2.5. Dimensionless values

In order to analyse these parameters in a synthetic way, it will be useful to define following dimensionless values, which we classify by type:

$$\tilde{T}_{\mathrm{a}}=\frac{T_{\mathrm{a}}}{\theta_{\mathrm{a}0}} \tag{58}$$

$$\tilde{t}=\frac{t}{\tau},\quad\Delta\tilde{t}=\frac{\Delta t}{\tau} \tag{59}$$

$$\tilde{r}_0=\frac{r_0}{\delta},\quad\Delta\tilde{R}_0=\frac{\Delta R_0}{\delta} \tag{60}$$

$$\tilde{S}=\frac{S}{S_{\delta}} \tag{61}$$

$$\tilde{h}_{\mathrm{s}}=\frac{h_{\mathrm{s}}}{h_{\delta}},\quad\tilde{k}_{\mathrm{s}}=\frac{k_{\mathrm{s}}}{h_{\delta}},\quad\tilde{h}_{\mathrm{a}}=\frac{h_{\mathrm{a}}}{h_{\delta}},\quad\tilde{h}=\frac{h}{h_{\delta}}$$
$$\tilde{k}=\frac{k}{h_{\delta}},\quad\Delta\tilde{h}=\frac{\Delta h}{h_{\delta}},\quad\Delta\tilde{k}=\frac{\Delta k}{h_{\delta}} \tag{62}$$

where S represents the air/tube exchange surface:

$$S=2\pi r_0x \tag{63}$$

and where, accordingly to (28)–(30), h_{δ} and S_{δ} are the diffusive exchange coefficient and associated characteristic surface for a steady signal, a soil layer of thickness δ and an infinite convection coefficient ($h=h_{\mathrm{s}}=h_{\delta}$):

$$h_{\delta}=\frac{\lambda_{\mathrm{s}}}{r_0\ln\left(1+\frac{\delta}{r_0}\right)} \tag{64}$$

$$S_{\delta}=\frac{c_{\mathrm{a}}\dot{m}_{\mathrm{a}}}{h_{\delta}} \tag{65}$$

With these definitions (52) finally reduces to:

$$\tilde{T}_{\mathrm{a}}=\exp(-\tilde{h}\tilde{S})\cdot\cos(2\pi(\tilde{t}-\Delta\tilde{t})-\tilde{k}\tilde{S}) \tag{66}$$

2.6. Diffusive coefficients h_s and k_s

By means of these reductions, the behaviour of the diffusive coefficients h_{s} and k_{s} in function of the soil thickness ΔR_0 reveals their physical meaning (Fig. 2).

In case of an isothermal boundary condition, increase of soil thickness ΔR_0 progressively isolates the

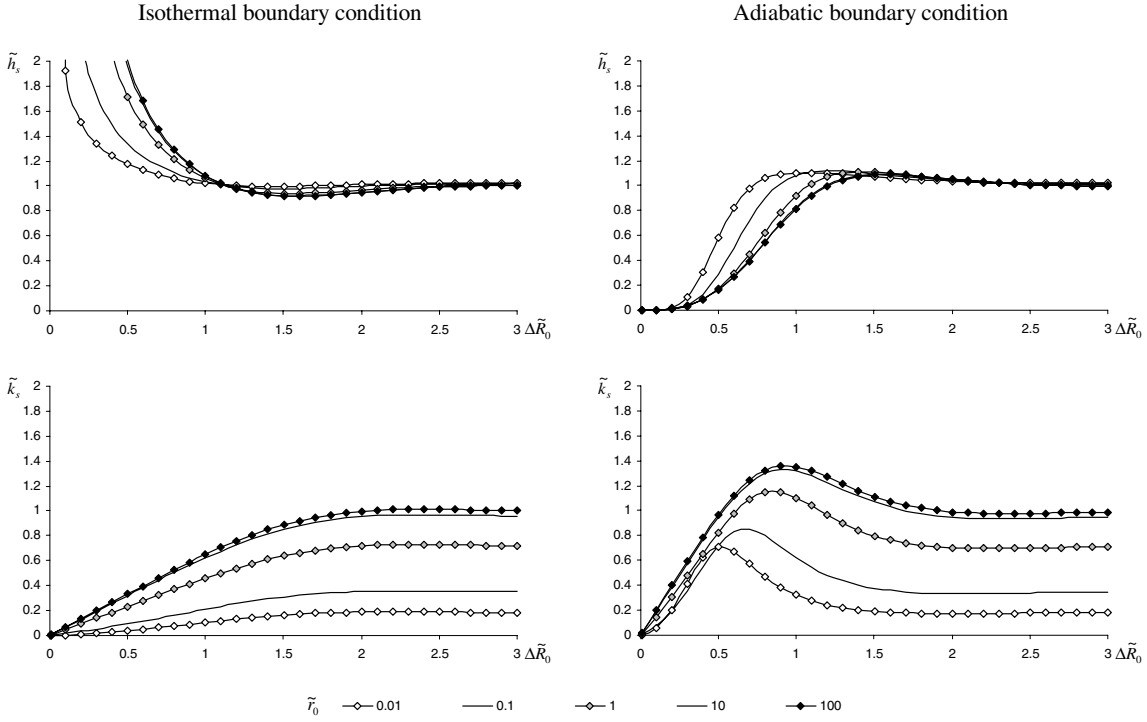

Fig. 2. Diffusive amplitude-dampening and phase-shifting coefficient in function of soil thickness and different pipe radius.

pipe from the temperature source at the surface, which translates by a decrease of dampening coefficient h_s (with the same logarithmic behaviour (28a) as for steady input). Latter coefficient however stabilises as the soil thickness exceeds δ, indicating that the active layer now restricts to the penetration depth, exceeding soil basically remaining unaffected by the temperature oscillation of the air.

A similar limitation by δ can be observed for an adiabatic boundary condition: above a thickness δ oscillatory behaviour of the input signal induces dampening just in the same manner as for an isothermal boundary condition (and much to the contrary of the flat behaviour (28b) of steady input). As a matter of fact, if the boundary condition is situated beyond the oscillatory penetration depth, there is no way for the air to "distinguish" whether latter condition is adiabatic or isothermal. Should the soil thickness ΔR_0 however drop below δ, then the dampening coefficient h_s would decrease and eventually vanish, indicating that the thermal capacity is being reduced, the limiting case being that of a perfectly isolated pipe with no active mass whatsoever.

Similar saturation phenomena appears for the phase-shifting coefficient k_s. For one or the other boundary conditions, latter rises along with ΔR_0 and stabilises as latter goes beyond penetration depth δ (in the case of an adiabatic boundary condition first going through a maximum point). To the contrary of the dampening coefficient h_s whose stabilising value is independent of the pipe radius (in dimensionless form!), that of k_s turns out to decrease along with the radius though.

2.7. Convective coupling and corrective coefficients Δh and Δk

In case of an adiabatic boundary condition, coupling with a finite convective coefficient h_a essentially acts by dividing the thermal potential, so that effective coefficients h and k basically behave like reduced forms of h_s and k_s (Fig. 3), which justifies formulation (49) and (50). When h_a decreases close to h_δ or smaller, corrective coefficients Δh and Δk can become quite important though (Fig. 4), especially for ΔR_0 smaller than δ. In latter case Δh will tend to linearise the power-behaviour of h in a way similar to that of k, which will perturb the phase-shifting phenomena put forward in next section.

Less important for subsequent considerations, similar discussion of the isothermal case is to be found in [15].

2.8. Flat heat-exchanger

By proper geometric modification of governing Eqs. (1)–(3), foregoing study can be extended to the case of a flat heat-exchanger (convection between an airflow and

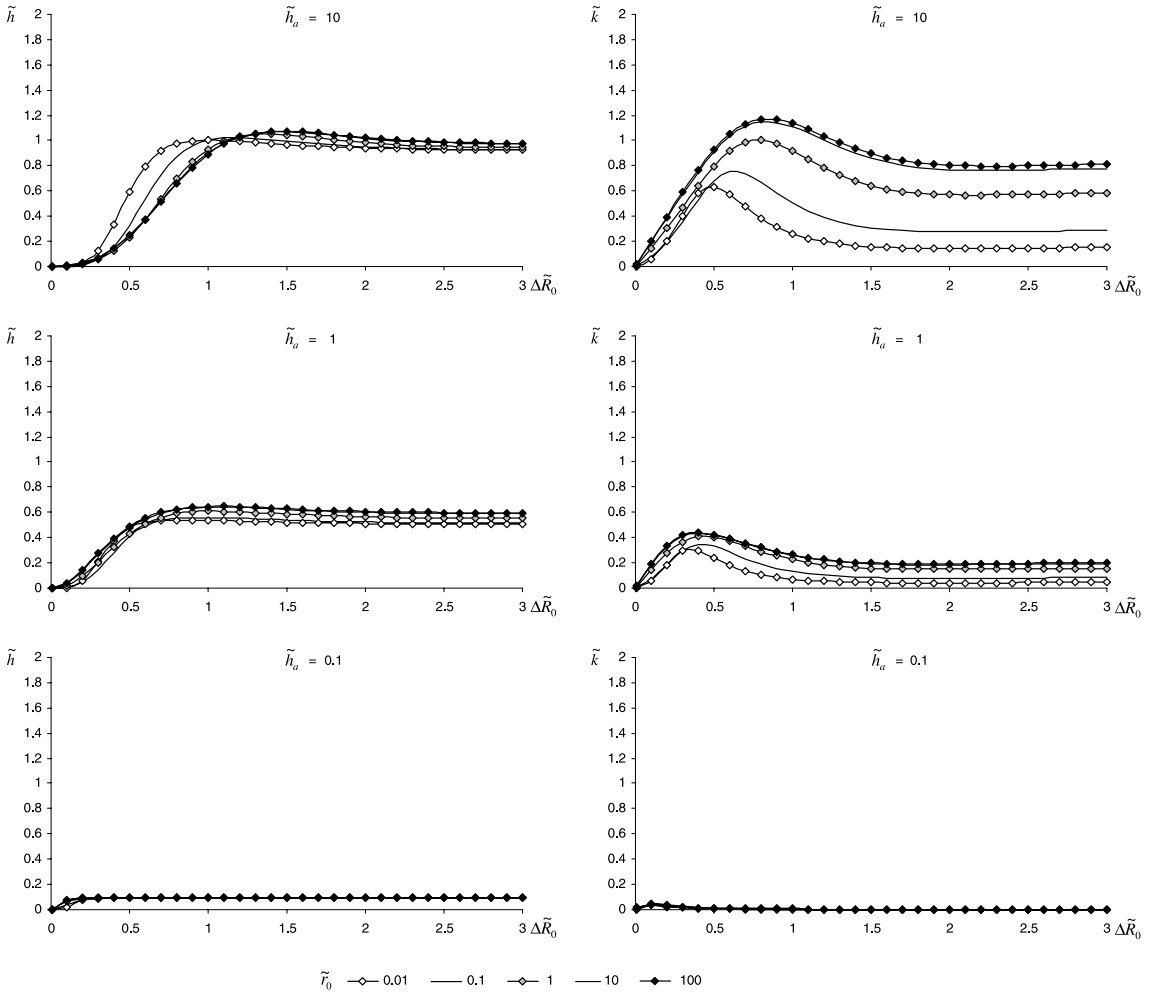

Fig. 3. Total amplitude-dampening and phase-shifting coefficient, adiabatic boundary condition.

a flat plate of length x, width y and finite thickness ΔR_0, with induced one-dimensional heat diffusion along r, perpendicular to airflow):

$$a_s \frac{\partial^2 T_s}{\partial r^2} = \frac{\partial T_s}{\partial t} \tag{67}$$

$$c_a \dot{m}_a \left(\frac{\partial T_a}{\partial x} + \frac{1}{v_a} \frac{\partial T_a}{\partial t} \right) = y h_a (T_s|_{r=0} - T_a) \tag{68}$$

$$\lambda_s \left. \frac{\partial T_s}{\partial r} \right|_{r=0} = h_a (T_s|_{r=0} - T_a) \tag{69}$$

For a harmonic input of type (33), resulting output air temperature turns out to be of equivalent form as (52):

$$T_a(x,t) = \theta_{a0} \cdot \exp\left(-\frac{Sh}{c_a \dot{m}_a} \right) \cdot \cos\left(\omega \left(t - \frac{x}{v_a} \right) - \frac{Sk}{c_a \dot{m}_a} \right) \tag{70}$$

where $S = xy$ represents the air/plate exchange surface. Coefficients h and k continue to be determined by (53)–(57), where h_Γ^* is now given as follows:

- With an isothermal boundary condition at ΔR_0:

$$h_\Gamma^* = \frac{\lambda}{\delta} \cdot (1+\mathrm{i}) \cdot \frac{\cosh\left((1+\mathrm{i})\frac{\Delta R_0}{\delta}\right)}{\sinh\left((1+\mathrm{i})\frac{\Delta R_0}{\delta}\right)} \tag{71a}$$

- With an adiabatic boundary condition at ΔR_0:

$$h_\Gamma^* = \frac{\lambda}{\delta} \cdot (1+\mathrm{i}) \cdot \frac{\sinh\left((1+\mathrm{i})\frac{\Delta R_0}{\delta}\right)}{\cosh\left((1+\mathrm{i})\frac{\Delta R_0}{\delta}\right)} \tag{71b}$$

Coherent with the fact that a flat heat exchanger actually corresponds to a finite portion of a hollow cylinder of thickness ΔR_0 and infinite radius r_0, expression

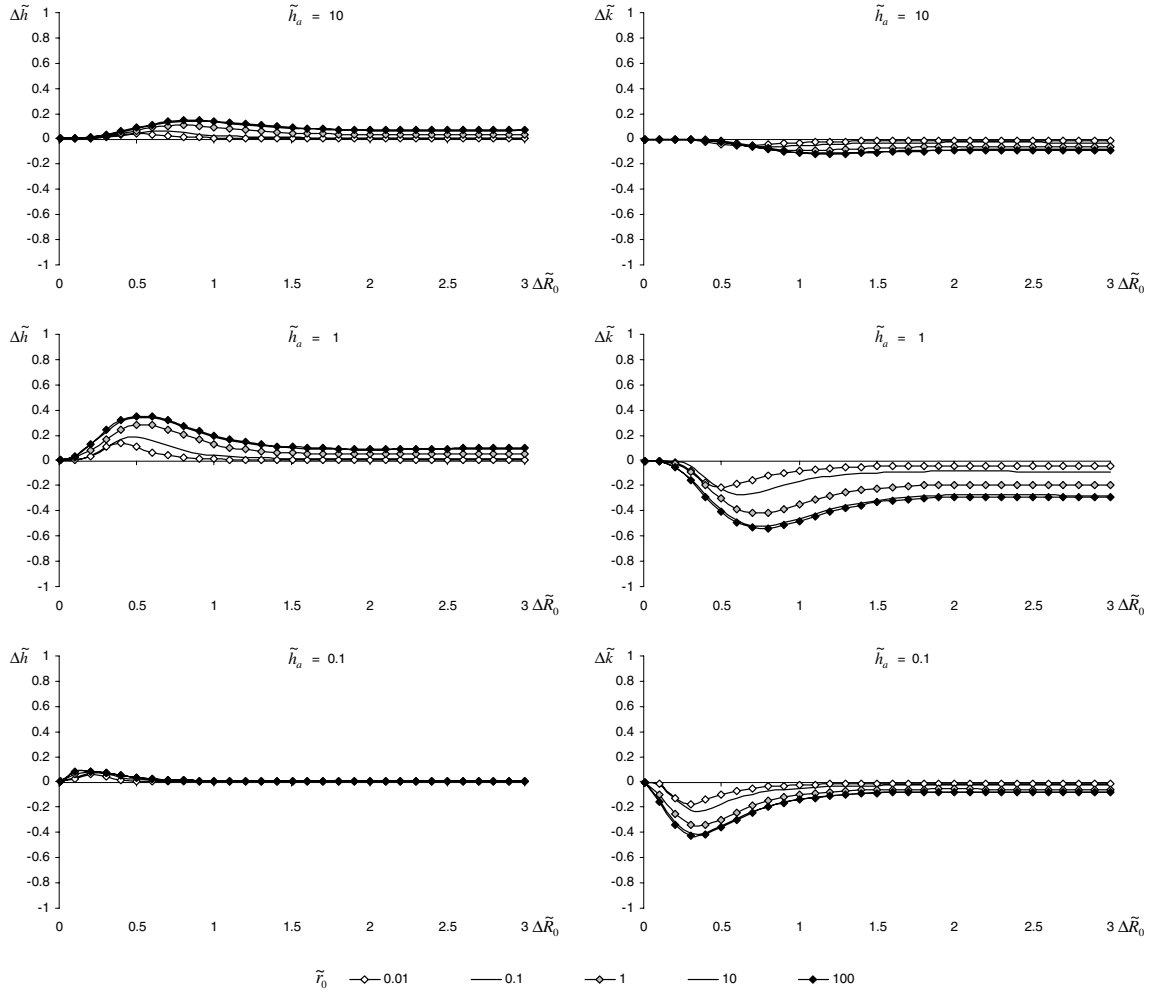

Fig. 4. Total amplitude-dampening and phase-shifting coefficient-correction, adiabatic boundary condition.

(71) actually turns out to coincide with the limiting form of Eq. (50), so that h_s and k_s can also be evaluated by means of Fig. 2 with $r_0 = 100\delta$.

3. Amplitude-dampening versus phase-shifting

Solution (52) or (70) clearly show the joint amplitude-dampening and phase-shifting a diffusive heat-exchanger exercises on an airflow with oscillatory input signal. We will now analyse the relative importance of these two effects, distinguishing soil layers sufficiently or insufficiently thick for heat diffusion to expand over all its natural depth.

3.1. Amplitude dampening by complete development of the active layer

With a sufficiently thick soil ($\Delta R_0 > \delta$) isothermal and adiabatic boundary conditions have been seen to have equivalent effects on the airflow temperature. The dampening coefficient h_s is then essentially equivalent to the dampening coefficient h_δ for a steady-state input and a soil of thickness δ, while the phase-shifting coefficient k_s generally remains below that value, which is only reached in the case of a flat exchanger. Compared to amplitude-dampening, phase shifting will thus become a relatively secondary phenomenon.

Hence (Fig. 5, left), for a flat exchanger and a sufficiently good convective coupling ($h_a > 10h_\delta$), an exchange surface $S = S_\delta$ will yield a phase shift of barely 1 rad (4 h in daily frequency, 2 months in annual frequency) for an amplitude dampening by a factor e^{-1}. Complete phase shifting of π (12 h, respectively 6 months) will only be reached when the amplitude already dampened down by a factor $e^{-\pi} \sim 4\%$. Other geometric cases will be characterised by an even smaller phase-shift, as k decreases along with the pipe radius as well as with the convective exchange h_a (Fig. 3).

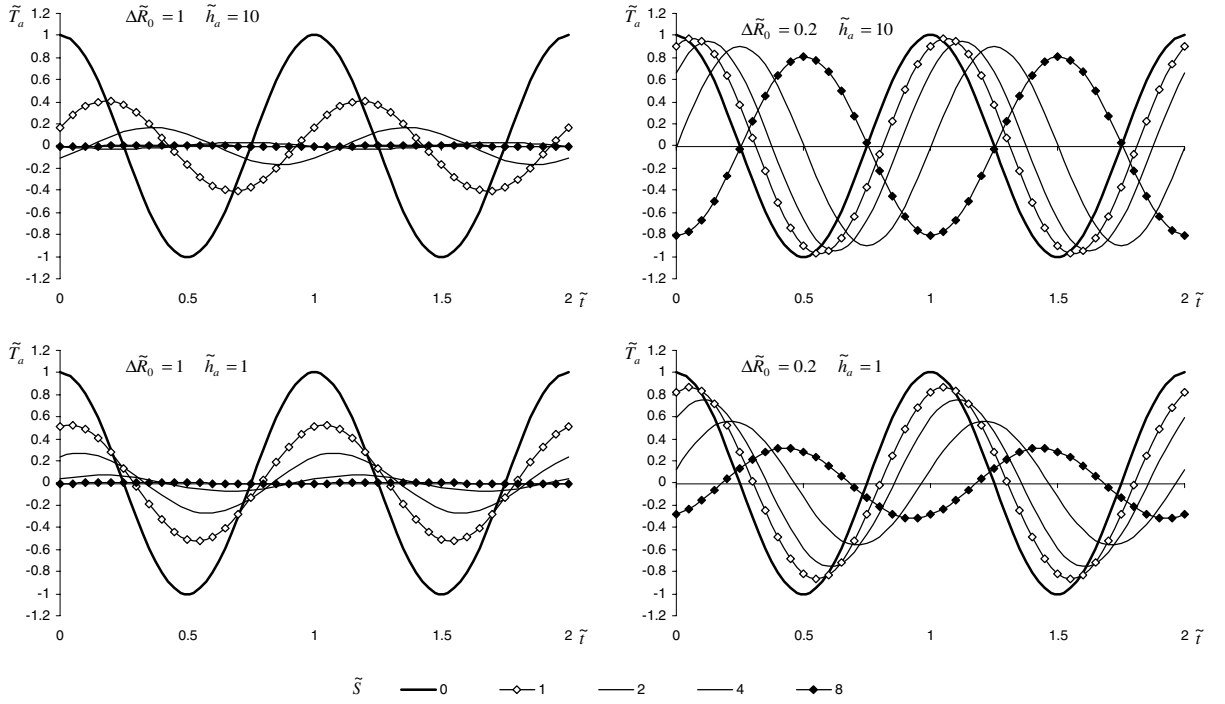

Fig. 5. Amplitude-dampening and phase-shifting of periodic input in flat air/soil heat-exchanger with adiabatic boundary condition.

3.2. Phase-shifting by development of a thin isolated layer

Only when the soil thickness reduces beneath δ will isothermal and adiabatic condition differ from each other. In the first case, the airflow entering in closer contact with the constant temperature source, amplitude dampening will turn out even stronger, to the contrary of phase-shifting which will decrease even more (Fig. 2).

For the adiabatic case, a completely new phenomenon will however appear. Although both diffusive coefficients then progressively drop to zero along with ΔR_0, k_s does it in a linear while h_s in a power form (Fig. 2). As a result, for a value of ΔR_0 close to 0.2δ there is a residual phase-shifting coefficient, all the more important as the pipe radius also is (up to $0.4h_\delta$ in case of a flat exchanger), for an almost extinguished dampening coefficient. Supposing a fairly good convective exchange it hence becomes possible, with such a thin and isolated layer configuration, to get a complete phase-shift of the input oscillation with almost no amplitude dampening (Fig. 5, right). As has been seen before, poor convective exchange however will linearise the form of h, amplitude-dampening becoming close to or stronger than phase-shifting again.

To the contrary of preceding amplitude-dampening regime (which is usually striven for when preheating or cooling of air by means of air/soil heat exchangers), this phase-shifting regime seems not to have been identified or intentionally used ever before.

4. Validation

4.1. Numerical simulation

First validation as well as illustration of the results just discussed will be given on the example of a theoretical air-to-earth heat exchanger used for preheating or cooling of air taken from ambient. Input is the standard annual meteorological data for Geneva as given in hourly time step by the Meteonorm database [23].

The analysed system is composed of a 25 cm diameter pipe embedded in a sandy and weakly saturated soil cylinder (conduction and capacity of 1.9 W/K m and 1.9 MJ/K m^3, yielding 17 cm and 3.2 m daily and annual penetration depths), with adiabatic boundary conditions and submitted to a constant 200 kg/h airflow (inducing a value of h_a of 4.6 W/K m^2). By Fourier analysis of the input temperature into a complete sum of harmonics (from yearly up to hourly frequence), the analytical output is being reconstructed for a set of three geometric configurations (Table 1), yielding respectively (Fig. 6): (a) dampening of annual amplitude, (b) dampening of daily amplitude and (c) phase-shifting of annual amplitude.

Table 1
Some configurations of cylindrical air/soil heat-exchangers with adiabatic boundary condition: amplitude-dampening and phase-shifting parameters as well as mean deviations from numerical simulation model

Configuration effect	R_0 (m)	x (m)	Parameters				Validation			
			Daily		Annual		Axial diffusion off		Axial diffusion on	
			$\tilde{S}\tilde{h}$	$\tilde{S}\tilde{k}$	$\tilde{S}\tilde{h}$	$\tilde{S}\tilde{k}$	Bias[a] (K)	Deviation[b] (K)	Bias[a] (K)	Deviation[b] (K)
Annual dampening	2.0	50	2.74	0.27	1.63	0.78	0.127	0.069	0.128	0.070
Daily dampening	0.6	50	2.73	0.27	0.05	0.36	0.080	0.043	0.080	0.042
Annual phase shift	0.6	400	21.8	2.17	0.42	2.89	0.489	0.171	0.488	0.167

[a] Mean difference (numerical – analytical).
[b] Square root of mean square difference (after deduction of bias).

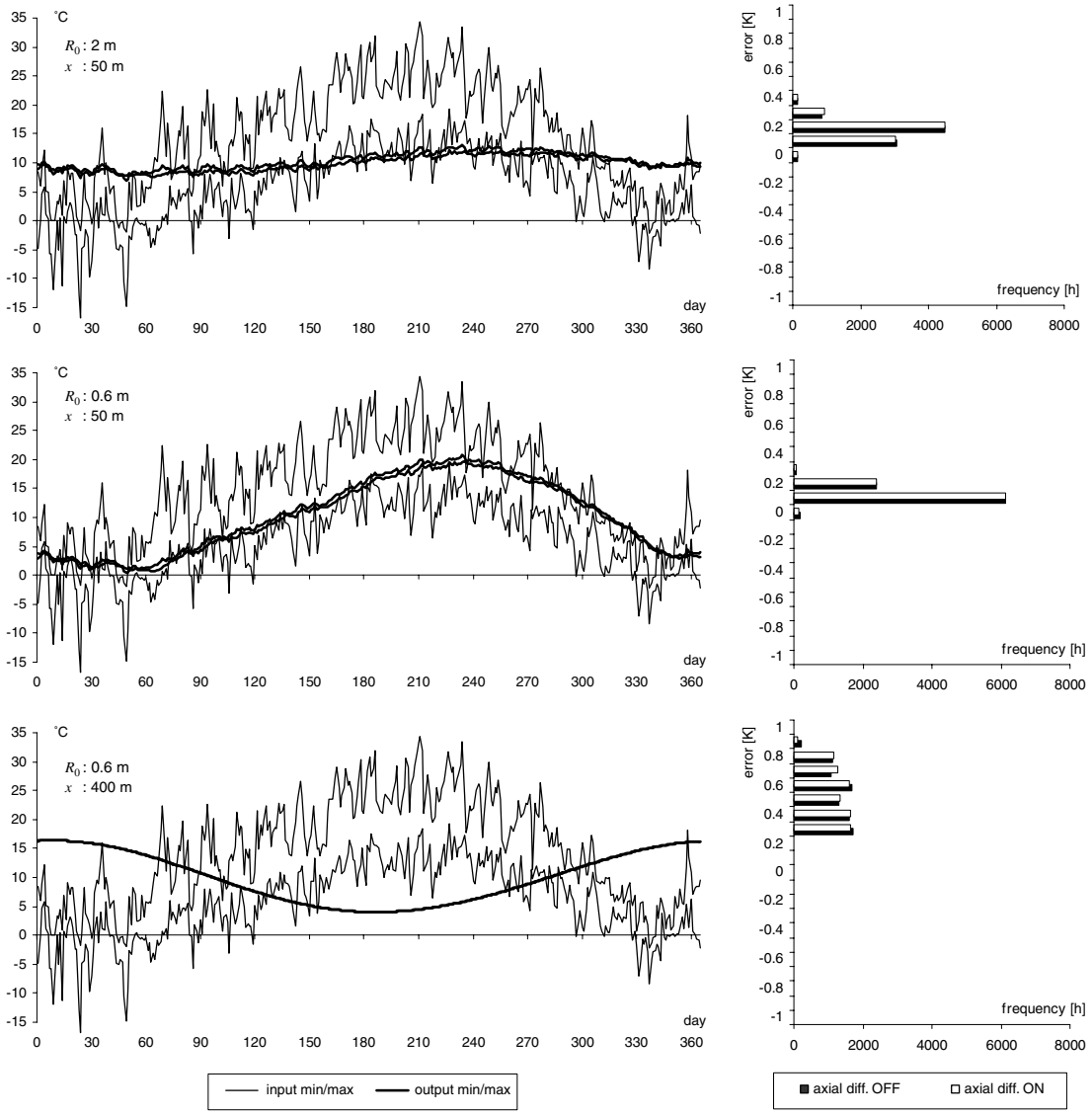

Fig. 6. Some configurations of cylindrical air/soil heat-exchangers with adiabatic boundary condition: daily extremes over one year for hourly input from ambient and analytically computed output (left) and hourly deviation from numerical simulation model (right).

Validation concerns output from a finite element simulation model previously developed by the author and briefly described in the introduction. Input temperature, airflow, overall convective exchange coefficient, as well as soil properties were set to same values as above. Rectangular meshing was chosen so as to yield equivalent cylindrical sections than analytical problem (at pipe as well as soil level). It was laterally submitted to adiabatic boundary condition and longitudinally segmented in 1 m pieces. Finally, so as to determine the effect of longitudinal heat diffusion, not taken into account in the analytical model, latter segments alternatively were or were not separated with a 10 cm superisolating layer (2.8×10^{-5} W/K m conductivity, 2.8 kJ/m^3 capacity).

Despite the rectangular approximation of the numerical model, an excellent correspondence with the analytical approach is manifest (Fig. 6 and Table 1), with a mean bias of at most 0.5 K and a standard deviation below 0.2 K. At least for these configurations, with characteristic lengths way higher than annual and daily penetration depths, weak effect of longitudinal diffusion is moreover testified by the quasi equivalence of numerical results with axial diffusion turned on or off.

4.2. Experimental setup

Preliminary experimental validation of 12 h phase-shifting was done on a flat heat exchanger (5 mm air strip between two corrugated concrete plates 3.4 cm thick, 25 cm large and 2 m long, with 12 cm lateral polystyrene insulation), submitted to an 8 m^3/h airflow (Fig. 7). At input, weak meteorological oscillation was boosted with a 12 h electrical heating pulse (Fig. 8).

Despite too weak a convective exchange (inducing non-negligible amplitude-dampening) and too small an exchange surface (inducing not more than an 8 h

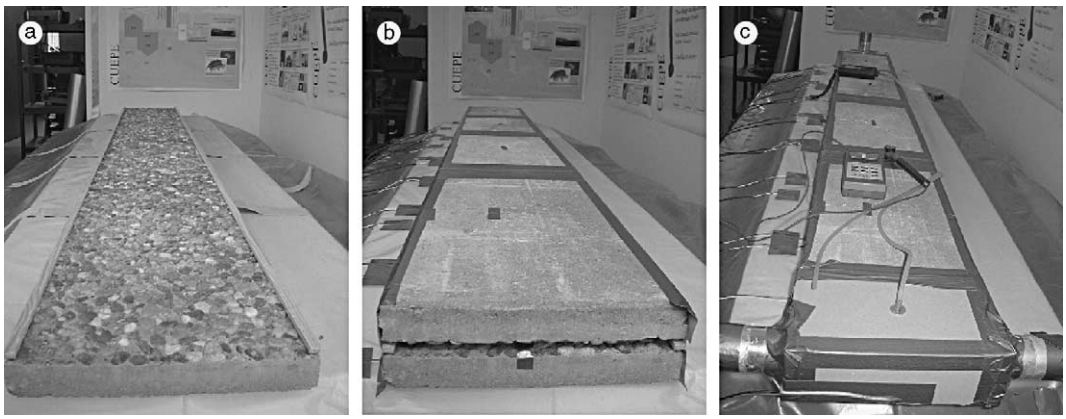

Fig. 7. Experimental setup for phase-shifting with controlled amplitude-dampening: (a) basis: washed concrete plate on polystyrene insulation; (b) air strip and second concrete plate; (c) finish (before lateral and upper insulation): air injection, air tightness and monitoring apparatus.

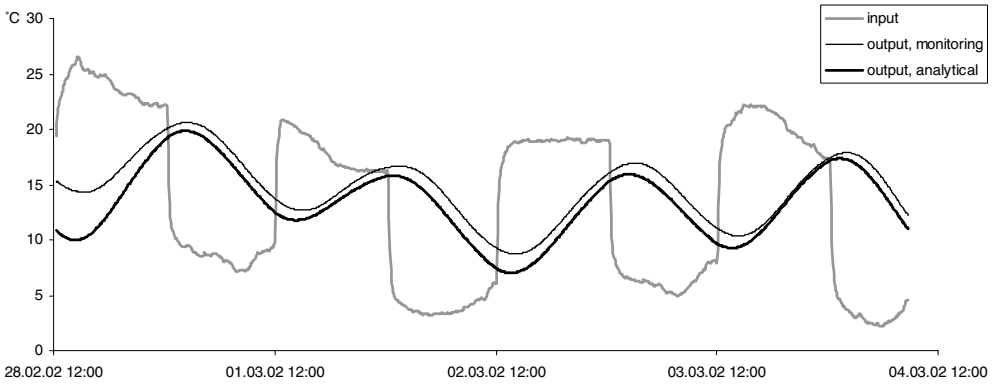

Fig. 8. Validation of phase-shifting with controlled amplitude-dampening.

phase-shift), there is clear evidence of the phenomenon striven for. This experiment furthermore shows the critical importance of the active layer, in present case chosen so as to phase-shift the fundamental frequency, while all higher frequencies of the "square" pulse are being dampened out.

Finally, monitored data can be fairly well reproduced by way of analytically reconstructed output (Fig. 8), having in mind that Fourier decomposition also assumes the repeated periodic pattern as a historical input. This analytical reconstruction however critically depends on the value of h_a, best results here being obtained with $h_a = 17 \pm 2$ W/K m^2 (for $\lambda_s = 1.5$ W/K m and $c_s = 2.6$ MJ/K m^3). Such an experimental setup could hence also be used for experimental determination of convective exchange coefficients, as here with corrugated plates.

5. Conclusions

We developed an analytical solution for a cylindrical (or flat) air/soil heat-exchanger submitted to constant airflow, with harmonic temperature input and adiabatic or isothermal boundary condition, yielding following results:

- Characterisation and physical interpretation of amplitude-dampening and phase-shifting phenomena which, depending on the available soil thickness, are subject to distinct regimes. Depending on the effect striven for and the frequency of interest, this characterisation sets up the basis for proper dimensioning of air/soil heat exchangers.
- Detection of the possibility to use a diffusive heat-exchanger for phase-shifting of a temperature oscillation, with almost no amplitude-dampening. Apparently unexploited up to now, this phenomena might give rise to interesting energy handling techniques, on air as well as may be on water driven systems. Yearly phase-shifting of ambient temperature as presented in this article probably would turn out to be technically unrealistic (size, adiabatic conditions) and should be perturbed by latent exchanges (as can be shown with numerical simulation taking into account air humidity). Daily phase-shifting for summer cooling purposes should however be an interesting option, on which work at the Centre universitaire d'étude des problèmes de l'énergie is currently being developed.
- Numerical validation on hourly data over one year confirms the analytical results and the coherence of subjacent assumptions, at least in the range of tested configurations. Experimental validation of daily phase-shifting, which also contributes to settle analytical results, could further be used for precise determination of effective convective heat exchange coefficient within air/soil heat-exchangers.

Acknowledgements

We wish to thank Bernard LACHAL from the Centre universitaire d'étude des problèmes de l'énergie for suggesting to treat the analytical problem of air/soil heat-exchangers and for constant and helpful discussions throughout the work, as well as for carrying out the experimental validation, in collaboration with Eric PAMPALONI. We also thank the Swiss Federal Office of Energy and the Geneva Cantonal Office of Energy for their financial contribution.

References

[1] M. Abramowitz, I. Stegun, Handbook of mathematical functions, National Bureau of Standards, Applied Mathematics Series, 55, 1972.
[2] A.K. Athienitis, M. Santamouris, A. Kyprianou, Application of ground cooling/heating for HVAC air precooling/preheating for the University of Cyprus, in: Architecture, city, environment, proceedings of PLEA 2000, Cambridge, UK, London, James & James, 2000, pp. 94–99.
[3] N.K. Bansal, M.S. Sodha, S.S. Bharadwaj, Performance of earth air tunnels, Energy Res. 7 (1983) 333–345.
[4] M. Bojic, N. Trifunovic, G. Papadakis, S. Kyritsis, Numerical simulation, technical and economic evaluation of air-to-earth heat exchanger coupled to a building, Energy 22 (12) (1997) 1151–1158.
[5] T. Boulard, E. Razafinjohany, A. Baille, Heat and water vapour transfer in agricultural greenhouse with an underground heat storage system, part 1 and 2, Agr. Forest Meteorol. 45 (1989) 175–194.
[6] B. Chen, T. Wang, J. Maloney, M. Newman, Measured and predicted cooling performance of earth contact cooling tube, in: Proceedings of ASES 1983 Annual Meeting, Minneapolis, MN, 1983.
[7] M. Chung, P.S. Jung, R.H. Rangel, Semi-analytical solution for heat transfer from a buried pipe with convection on the exposed surface, Int. J. Heat Mass 42 (1999) 3771–3786.
[8] J. Claesson, A. Dunand, Heat extraction from the ground by horizontal pipes: a mathematical analysis, Stockholm, Swedish Council for Building Research, 1983.
[9] M. De Paepe, Three dimensional time accurate unstructured finite volume technique for modelling ground-coupled heat exchangers, in: Proceedings of HEFAT'2002, 1st International Conference on Heat Transfer, Fluid Mechanics and Thermodynamics, Satara Kamp, Kruger National Park, South Africa, 2002.
[10] D. Elmer, G. Schiller, A preliminary examination of the dehumidification potential of earth/air heat exchangers, in: Proceedings of the 1st National Passive Cooling Conference, Miami, 1981, pp. 161–165.

[11] C. Gauthier, M. Lacroix, H. Bernier, Numerical simulation of soil heat exchanger-storage systems for greenhouses, Solar Energy 30 (6) (1997) 333–346.
[12] V. Gnielinski, Neue Gleichungen für den Wärme- und den Stoffübergang in turbulent durchströmten Rohren und Kanälen, Forsch. Ing.-Wes. 41 (1) (1975) 8–15.
[13] W. Gygli, K. Fort, Trnsys-model type 60 for hypocaust thermal storage and floor heating, User manual (available at the author's address: Karel Fort, Chimligasse 14, CH-8603 Schwerzenbach), 1994.
[14] P. Hollmuller, B. Lachal, Cooling and preheating with buried pipe systems: monitoring, simulation and economic aspects, Energy Buildings 33/5 (2001) 509–518.
[15] P. Hollmuller, Utilisation des échangeurs air/sol pour le chauffage et le rafraîchissement des bâtiments. Mesures in situ, modélisation analytique, simulation numérique et analyse systémique, Ph.D. Thesis, Université de Genève, 2002, p. 125.
[16] A. Huber, S. Remund, Wiederstands-Kapazitäten-Model WKM_Lte: Program for the simulation of air-earth heat exchangers, Huber Energietechnik, Zürich, 1996.
[17] V.P. Kabashnikov, L.N. Danilevskii, V.P. Nekrasov, I.P. Vityaz, Analytical and numerical investigation of the characteristics of a soil heat exchanger for ventilation systems, Int. J. Heat Mass 45 (2002) 2407–2418.
[18] M. Koschenz, B. Lehmann, Thermoaktive Bauteilsysteme tabs, Dübendorf, EMPA, 2000.
[19] F. Incropera, D. De Witt, Fundamentals of Heat and Mass Transfer, third ed., John Wiley & Sons, 1990.
[20] H.J. Levit, R. Gaspar, R.D. Piacentini, Simulation of greenhouse microclimate by earth-tube heat exchangers, Agr. Forest Meteorol. 47 (1989) 31–47.
[21] X. Luo, W. Roetzel, U. Lüdersen, The single-blow transient testing technique considering longitudinal core conduction and fluid dispersion, Int. J. Heat Mass Transfer 44 (2001) 121–129.
[22] X. Luo, W. Roetzel, The single-blow transient testing technique for plate-fin heat exchangers, Int. J. Heat Mass Transfer 44 (2001) 3745–3753.
[23] METEONORM Version 2.0, database and simulation software for solar energy, Infoenergie, CH-5200 Brugg, 1995.
[24] G. Mihalakakou, M. Santamouris, D. Asimakopoulos, Modeling the thermal performance of earth-to-air heat exchangers, Solar Energy 53 (3) (1994) 301–305.
[25] E.A. Rodriguez, J.M. Cjudo, S. Alvarez, Earth-tube systems performance, in: Proceedings of CIB Meeting on Air Quality and Air Conditioning, Paris, France, 1988.
[26] M. Santamouris, C.C. Lefas, Thermal analysis and computer control of hybrid greenhouse with subsurface heat storage, Energy Agr. 5 (1986) 161–173.
[27] R.L. Sawhney, U. Mahajan, Heating and cooling potential of an underground air-pipe system, Int. J. Energy Res. 18 (1994) 509–524.
[28] G. Schiller, Earth tubes for passive cooling, the development of a transient numerical model for predicting the performance of earth-to-air heat exchangers, M.Sc. thesis, MIT, Mechanical Engineering, 1982.
[29] A.L.T. Seroa da Motta, A.N. Young, The predicted performance of buried pipe cooling systems for hot humid climates, in: E. Bilgen, K.G.T. Hollands (Eds.), Proceedings of Intersol'85, 1985, pp. 759–770.
[30] L. Serres, A. Trombe, J.H. Conilh, Study of coupled energy saving systems sensitivity factor analysis, Build. Environ. 32 (2) (1997) 137–148.
[31] G.N. Tiwari, N. Lugani, A.K. Singh, Design parameters of a non-air-conditioned cinema hall or thermal comfort under arid-zone climatic conditions, Energy Build. 19 (1993) 249–261.
[32] A. Tzaferis, D. Liparakis, M. Santamouris, A. Argiriou, Analysis of the accuracy and sensitivity of eight models to predict the performance of earth-to-air heat exchangers, Energy Build. 18 (1992) 35–43.